

# Search for Single Top Production at LEP via FCNC at $\sqrt{s} = 189 - 207$ GeV

V.Obraztsov, S.Slabospitsky and O.Yushchenko

IHEP, Protvino, Russia

S. Andringa, P. Gonçalves, A. Onofre, L. Peralta,  
M. Pimenta and B. Tomé

LIP-IST-FCUL, Av. Elias Garcia, 14, 1, P-1000 Lisboa, Portugal

## Abstract

A search for Flavour Changing Neutral Currents is performed using data taken by the DELPHI detector at LEP-II. The data analysed were accumulated at the centre-of-mass energies ranging from 189 to 207 GeV. A limit at 95% confidence level was obtained on the parameters of the anomalous couplings  $\kappa_\gamma$  and  $\kappa_Z$ .



# 1 Introduction

Flavour Changing Neutral Currents (FCNC) are known to be absent at tree level in the Standard Model but can naturally appear at one-loop level due to CKM mixing. The relative suppression of the loop contributions together with the smallness of the non-diagonal CKM matrix elements ensures only small contributions to FCNC from the SM [1]. On the other hand many extended models such as supersymmetry [2] and multi-Higgs doublet models [3] predict the presence of FCNC already at tree level. Some specific models [4] give rise to detectable FCNC amplitudes.

The most prominent signature for direct observation of FCNC processes is the production of top quark together with light quark in the reaction  $e^+e^- \rightarrow \bar{t}c, \bar{t}u$ <sup>1</sup>.

The strength of the transitions  $\gamma \rightarrow f\bar{f}'$  and  $Z \rightarrow f\bar{f}'$  can be described in terms of the Lagrangian given in [5]:

$$\Gamma_\mu^\gamma = \kappa_\gamma \frac{ee_q}{\Lambda} \sigma_{\mu\nu} (g_1 P_l + g_2 P_r) q^\nu, \quad (1)$$

$$\Gamma_\mu^Z = \kappa_Z \frac{e}{\sin 2\Theta_W} \gamma_\mu (z_1 P_l + z_2 P_r) q^\nu, \quad (2)$$

where  $\Lambda$  is the new physics cutoff,  $e$  is the electron charge,  $e_q$  the top quark charge and  $\Theta_W$  is the weak mixing angle. The relative contributions of the left- and right components of the currents ( $g_i$  and  $z_i$ ) obey the constraints:

$$g_1^2 + g_2^2 = 1, \quad z_1^2 + z_2^2 = 1.$$

To estimate the parameters  $\kappa_\gamma$  and  $\kappa_Z$  one can consider the situation when the interference term that depend on  $g_i$  and  $z_i$  parameters becomes negative and decreases the cross section of the process  $e^+e^- \rightarrow t\bar{c}$ . This corresponds to the requirement [5]:

$$g_1 z_1 + g_2 z_2 = -1$$

The energy of the last LEP runs ( $\sqrt{s} = 189 - 207$  GeV) is well above the  $tc$  production threshold and gives the possibility to perform a direct search for FCNC. The advantage of this specific FCNC process consists in the fact that the  $t$ -quark can decays dominantly into  $Wb$ . This can produce some distinct signatures both in leptonic and hadronic  $W$  decay modes. Numerical estimations for the expected number of events taking into account the limits on anomalous vertices recently set by the CDF collaboration [6] can be found in [5].

One can get an almost background-free signature for the decays  $W \rightarrow l\nu$ , while the branching ratio is relatively low. The hadronic  $W$  decays give about three times higher event rate while the background situation is less favourable.

This note is devoted to the search of FCNC processes with an intermediate  $t$ -quark and subsequent  $W$  decay into quarks and leptons. The data were collected with the DELPHI detector [7] at  $\sqrt{s} = 189 - 207$  GeV and the statistics corresponds to a integrated luminosity of  $157.4 \text{ pb}^{-1}$  at 189 GeV,  $25.9 \text{ pb}^{-1}$  at 192 GeV,  $76.4 \text{ pb}^{-1}$  at 196 GeV,  $83.4 \text{ pb}^{-1}$  at 200 GeV,  $40.1 \text{ pb}^{-1}$  at 202 GeV and  $163.1 \text{ pb}^{-1}$  at 205 - 207 GeV.

---

<sup>1</sup>Throughout this paper the notation “c-quark” is used for both c- and u-quarks and the respective charge conjugation contribution also.

## 2 Hadronic Channel

In this analysis the events were preselected according to the standard hadronic selections described in [8]. An additional cut was applied to suppress events with an energetic muon or electron: the events with leptons above 20 GeV identified as (at least) *standard* electrons or *loose* muons (according to the classification described in [7]) were removed.

After that the LUCLUS algorithm with  $D_{join} = 6.5$  has been applied to perform the event clusterization into jets. Only events with 4, 5, or 6 jets have been selected and have been forced into a 4-jet topology. Each of the three most energetic jets should contain at least one charged track.

The jet assignment to quarks is not straightforward as the kinematics of the event strongly varies with the energy. The energies of the  $W$ -boson, the  $c$ - and  $b$ -quarks are given by the following expressions:

$$\begin{aligned} E_b &\simeq \frac{m_t^2 - m_W^2}{2m_t} \\ E_c &\simeq \frac{\sqrt{s}}{s} \left(1 - \frac{m_t^2}{s}\right) \\ E_W &\simeq \frac{m_t^2 + m_W^2 - m_b^2}{2m_t} \end{aligned}$$

One can observe that the assignment of the softest jet as  $c$ -jet that works quite well at the kinematic threshold of the single-top production can fail at highest LEP2 energies because the expected  $E_c \simeq 30$  GeV becomes compatible with the energies of the jets originating from the hadronic decay of the  $W$ .

Four different methods of jet assignment can be considered:

1. the jet with highest  $b$ -tag is the  $b$ -jet and the softest jet is the  $c$ -jet;
2. the most energetic jet is the  $b$ -jet and the softest jet is the  $c$ -jet;
3. the jet with highest  $b$ -tag is the  $b$ -jet and the 2jets  $\rightarrow W$  assignment is based on the best probability of the kinematic fit;
4. the most energetic jet is the  $b$ -jet and the 2jets  $\rightarrow W$  assignment is based on the best probability of the kinematic fit.

All the above methods have been studied and it was observed that the highest efficiency for the signal and strongest suppression for background can be achieved for the first method.

The pre-selection stage is finished by the requirement that the visible energy of the event  $E_{vis}$  is greater than 130 GeV. After that energies and momenta of jets are rescaled by applying a four-constraint fit.

The further analysis is based on a likelihood ratio method. Eight individual variables were chosen to construct the probability density functions:

- 1 global  $b$ -tag ( $b_{tag}$ ) calculated with the combined algorithm [9];

- 2 the invariant mass of two quarks assigned as jets originating from  $W$  hadronic decay ( $M_W$ );
- 3 the ratio of the energies of the softest and most energetic jets ( $E_{\min}/E_{\max}$ );
- 4 the energy of the jet assigned as b-jet ( $E_b$ );
- 5 the sphericity of the event;
- 6 the energy of the most energetic jet in the event ( $E_{\max}$ );
- 7 the momentum of the reconstructed  $W$  ( $P_W$ );
- 8 the thrust value.

Examples of the appropriate distributions are shown in figures 1 and 2.

The probability density functions were constructed for the individual signal and background distributions and the discriminating variable

$$W = \log \left( \prod_{i=1}^8 P_i^{\text{signal}} \right) - \log \left( \prod_{i=1}^8 P_i^{\text{backgr}} \right)$$

was calculated for every event. An example of this distribution is shown in figure 3 for signal events as well as real and MC WW events. The bottom-right plot shows the number of accepted real events as a function of the signal efficiency. One can observe a good agreement with MC prediction shown by curve.

The number of data events (and expected background from Standard Model simulation) which pass the likelihood ratio selection is shown in Table 1 for all centre of mass energies together with the signal efficiency.

$\sqrt{s}$ GeV	Lum. $\text{pb}^{-1}$	Eff. (%)	Expected	Observed
189.	157.4	16.4	29.75	29
192.	25.9	17.4	3.18	3
196.	76.4	16.3	10.93	14
200.	83.4	16.5	11.55	12
202.	40.1	16.4	5.60	5
206.	163.1	16.4	25.24	21

Table 1: Number of observed and expected events for the hadronic channel for the different centre of mass energies.

The numbers of observed events are in good agreement with the Standard Model expectations.

### 3 Semileptonic Channel

In the semileptonic channel the final state corresponding to the single top production, is characterized by two jets and at least one well isolated lepton (from the  $W$  leptonic

decay). Typically one of the jets is energetic (assumed to come from the  $b$ -quark) and the other one (assumed to come from the  $c$ -quark) is of low momentum.

In order to improve the selection efficiency a discriminating type of analysis was used to identify the semileptonic signal. At the pre-selection level the topology of the events was classified according to the number of jets, isolated leptons and photons. The events were accepted if they had at least 6 good tracks and at least one charged lepton (with hits on the vertex detector). All other particles (not including the isolated lepton) were forced into two jets by using the Durham jet algorithm [10]. It was additionally required that:

- the event visible energy had to be higher than 20% of the centre of mass energy;
- the momentum of the lepton and the most energetic jet had to be higher than 5 GeV/c;
- the polar angles of the lepton and the jets had to be above  $20^\circ$  and below  $160^\circ$ ;
- the polar angle of the missing momentum had to be above  $20^\circ$  and below  $160^\circ$ ;
- the impact b-tag parameter [9] was required to be less than 0.3.

The energies and momenta of the jets and the lepton were rescaled by a four-constraint fit. Events with  $\chi^2$  lower than 7 were accepted, provided the mass of the two jets and the mass reconstructed with the missing momentum and the isolated lepton momentum were both below  $100 \text{ GeV}/c^2$ .

After the pre-selection level and at an average centre of mass energy of  $\sqrt{s} = 189, 192, 196, 200, 202$  and  $205\text{-}207 \text{ GeV}$ , were found on data (are expected from SM simulation)  $271(269.3 \pm 6.5)$ ,  $57(45.7 \pm 1.1)$ ,  $172(137.7 \pm 3.2)$ ,  $179(144.4 \pm 3.5)$ ,  $85(69.6 \pm 1.7)$ , and  $253(277.9 \pm 7.1)$  respectively.

Figure 4 shows after the pre-selection level and for centre of mass energies ranging from 205 to 207 GeV the momentum of the most energetic jet and lepton and the angle between them.

After the pre-selection level a discriminating variable is constructed by using the distributions of the low energetic jet momentum, the combined event b-tag variable, the two jet reconstructed mass, the reconstructed top mass, the angle between the two jets and the lepton-neutrino (missing momentum) mass. For each event a signal likelihood ( $P_S$ ) and background likelihood ( $P_B$ ) probability is computed and the discriminating variable is defined as  $\log(P_S/P_B)$ .

Figures 5, 6 and 7 show some distributions at the pre-selection level.

Figure 8 represents the discriminating variable distribution and the number of events which are accepted in function of the discriminating variable cut. There is generally good agreement between the data and the Standard Model predictions.

Table 2 shows the number of events which pass a cut on the discriminating variable of 1.5 for the different centre of mass energies. The efficiencies convoluted with the  $W$  leptonic branching ratio are also shown.

$\sqrt{s}(\text{GeV})$	Data	Back.	$\epsilon \times \Gamma(W \rightarrow l^\pm \nu) \%$
189	4	$(2.8 \pm 0.8)$	$8.5 \pm 0.3$
192	1	$(0.5 \pm 0.1)$	$7.1 \pm 0.8$
196	2	$(0.9 \pm 0.3)$	$8.2 \pm 0.3$
200	3	$(0.8 \pm 0.3)$	$8.2 \pm 0.3$
202	1	$(0.4 \pm 0.1)$	$7.0 \pm 0.3$
205 – 207	1	$(2.0 \pm 0.6)$	$6.0 \pm 0.3$

Table 2: Number of events which pass a cut on the discriminating variable of 1.5 for the different centre of mass energies. The efficiencies convoluted with the  $W$  leptonic branching ratio are also shown.

## 4 Results and Conclusion

The combination of the data collected with the DELPHI detector at centre of mass energies ranging from 189 to 207 GeV in the hadronic and semileptonic channels results in upper limits on the anomalous Lagrangian parameters  $\kappa_\gamma$  and  $\kappa_Z$ . Due to the s-channel dominance the LEP2 data are less sensitive to the  $\kappa_\gamma$  parameter in comparison with  $\kappa_Z$ . Figure 9 shows in the  $\kappa_\gamma$  and  $\kappa_Z$  plane the 95% confidence level limit obtained by this analysis. The top FCNC decay widths were properly taken into account. The areas correspond to different top mass values. A visible improvement is obtained on the limits derived, when compared to the ones obtained at separate energies.

## References

- [1] Grzadkowski B, Gunion J.F., and Krawczyk P., *Phys. Lett.* **B268** (1991) 106;  
Eilam G, Hewett J.L, and Soni A., *Phys. Rev.* **D44** (1991) 1473;  
Luke M. and Savage M.J., *Phys Lett.* **B307** (1993) 387.
- [2] G.M.Divitiis, R.Petronzio, and L.Silvestrini, hep-ph/9704244 (1997).
- [3] D.Atwood, L.Reina, and A.Soni, SLAC-PUB-95-6927 (1995).
- [4] Arbuzov B.A. and Osipov M.Yu., hep-ph/9802392 (1998).
- [5] Obraztsov V.F., Slabospitsky S.R. and Yushchenko O.P., *Phys. Lett.* **B426** (1998), 393.
- [6] CDF Coll., Abe F. et al., FERMILAB-Pub-97/270-E, 1997.
- [7] DELPHI coll., P. Aarnio et al., Nucl. Instr. Meth. **A303** (1991) 233;  
DELPHI Coll., P. Abreu et al., Nucl. Instr. Meth. **A378** (1996) 57.
- [8] DELPHI Coll., P.Abreu et al., *Phys. Lett.* **B393** (1997) 245.
- [9] G. Borisov, C. Mariotti, DELPHI 97-16 PHYS672; DELPHI Coll., P. Abreu et al., Nucl. Inst. Meth. **A378** (1996) 57.
- [10] S. Catani et al., Phys. Lett. **B269** (1991) 432.



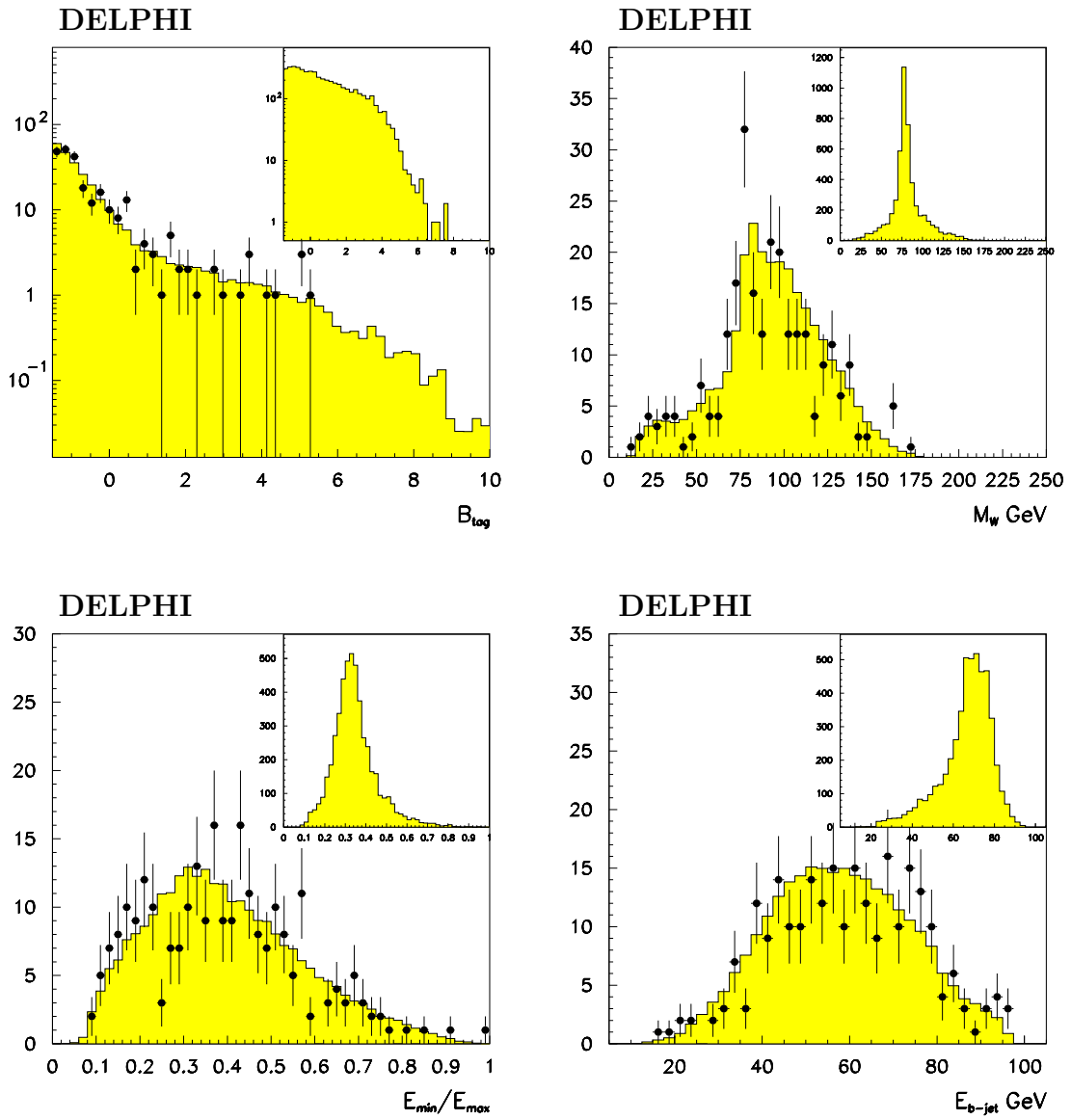


Figure 1: Distributions for hadronic  $W$  decay after pre-selections at  $\sqrt{s} = 200$  GeV. The signal distribution is shown in the upper right corners.

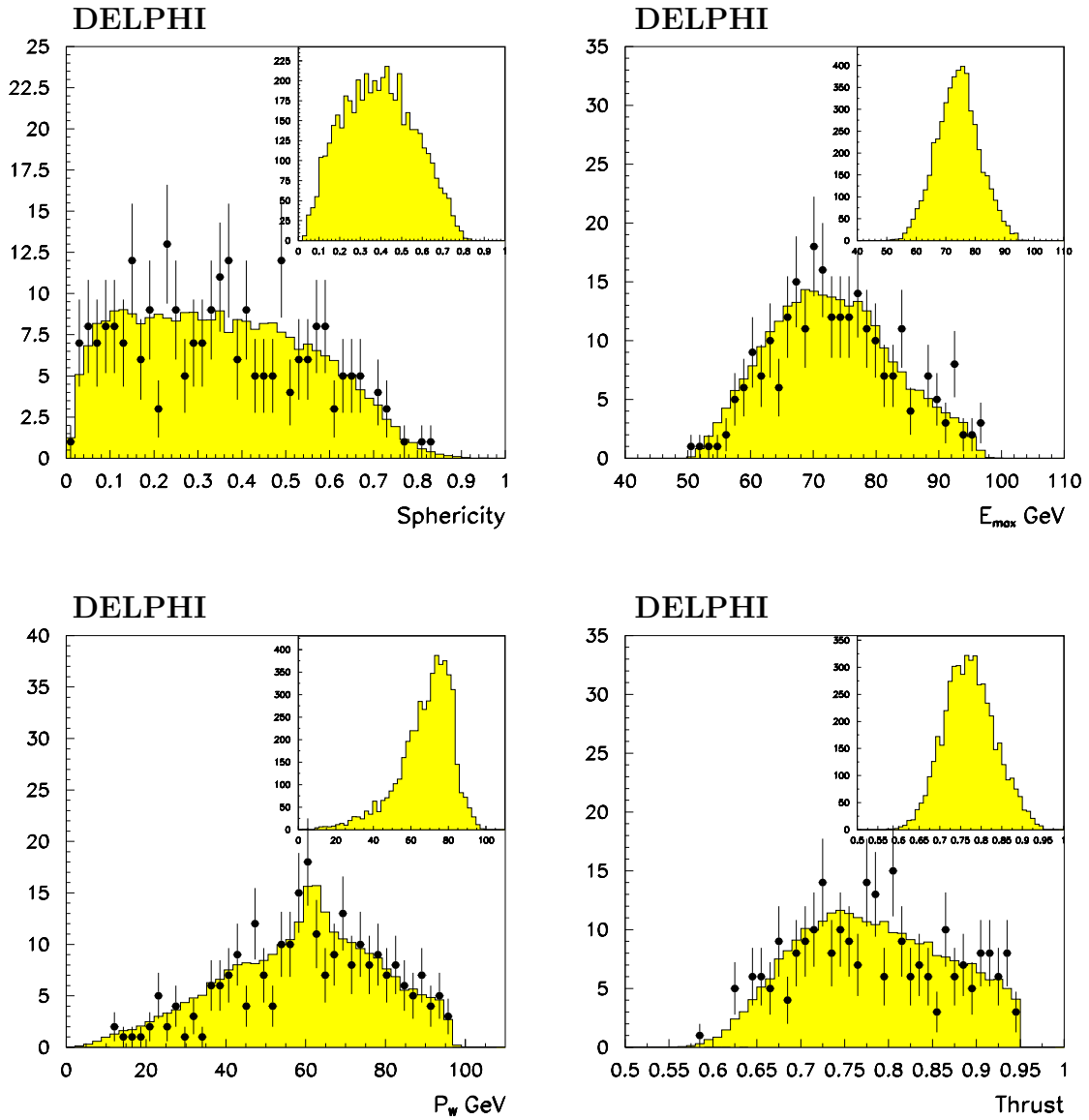


Figure 2: Distributions for hadronic  $W$  decay after pre-selections at  $\sqrt{s} = 200$  GeV. The signal distribution is shown in the upper right corners.

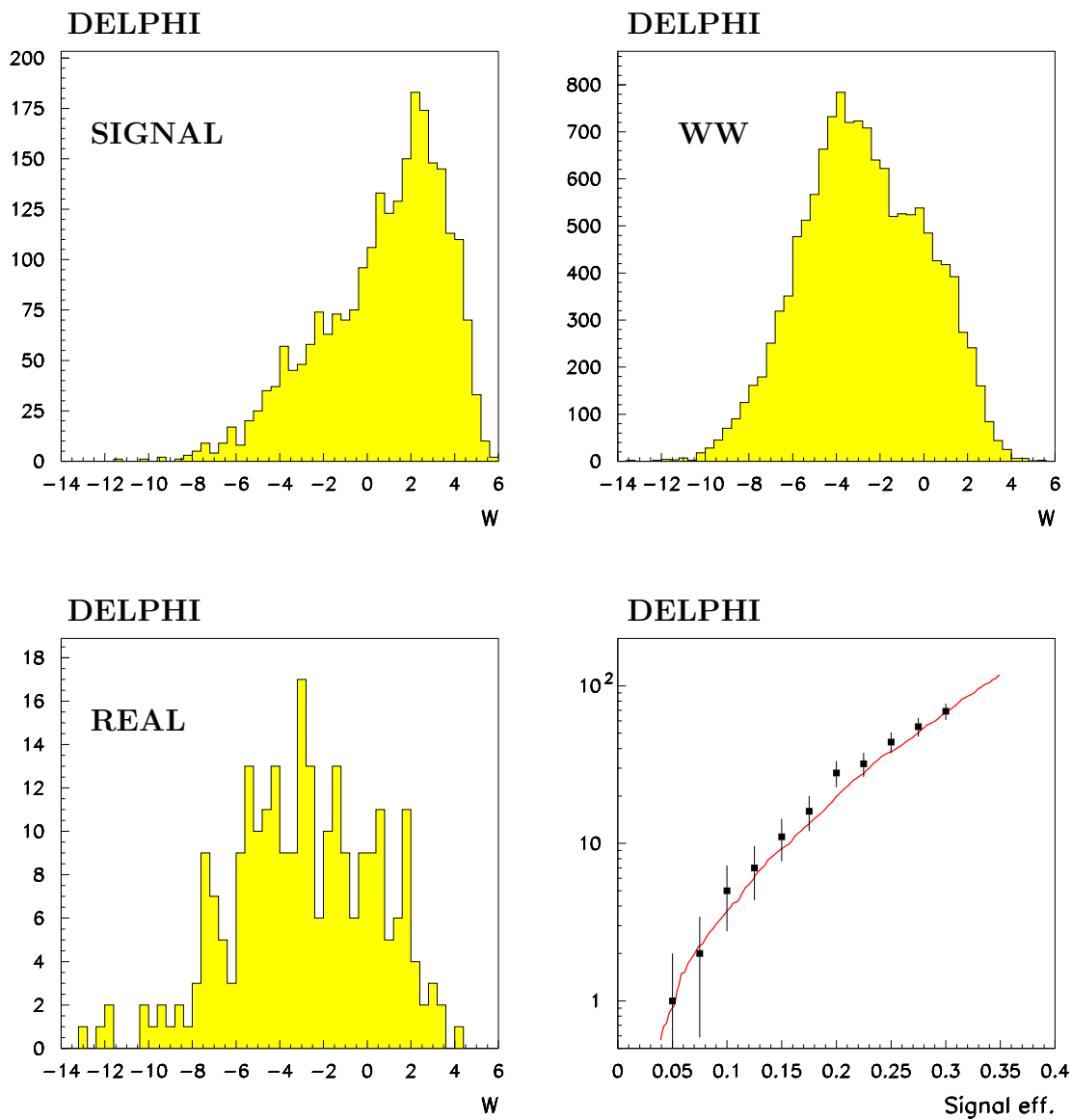


Figure 3: Distributions for discriminating variable at  $\sqrt{s} = 200$  GeV. The bottom-right plot shows the number of accepted real events as a function of the signal efficiency. The curve shows MC prediction.

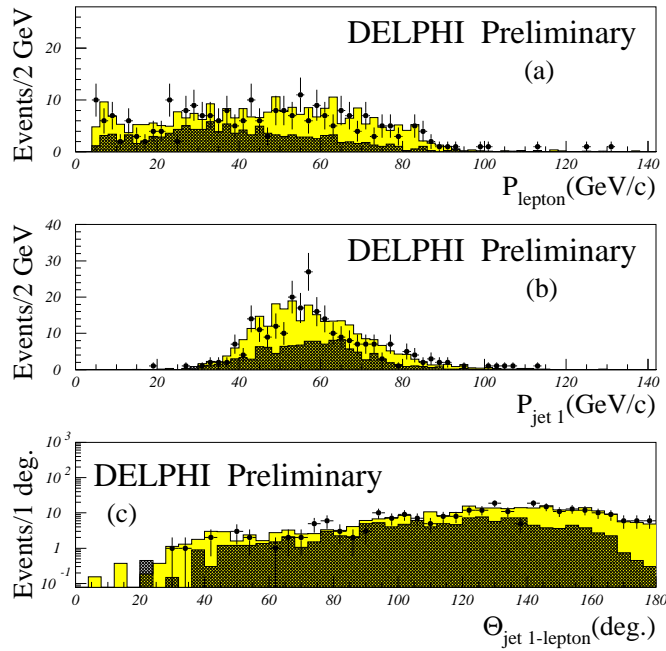


Figure 4: The most energetic lepton momentum (a), the most energetic jet momentum (b) and the angle between them, at a centre of mass energy in the range between 205-207 GeV. The dots show the data, the shaded region the SM simulation and the dark region the expected signal behaviour.

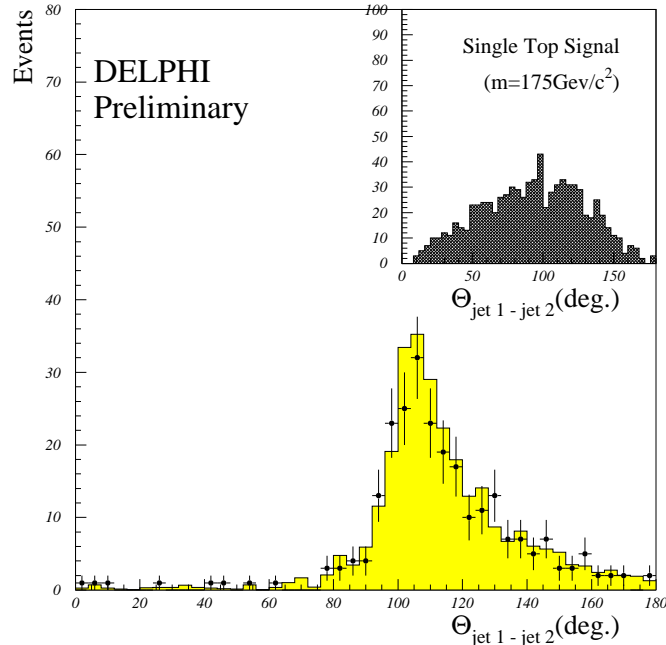


Figure 5: The angle between the two jets for the semileptonic decay channel, at a centre of mass energy in the range between 205-207 GeV. The dots show the data, the shadowed region the SM background and the top right distribution a signal of a top with a mass of 175 GeV/c<sup>2</sup>.

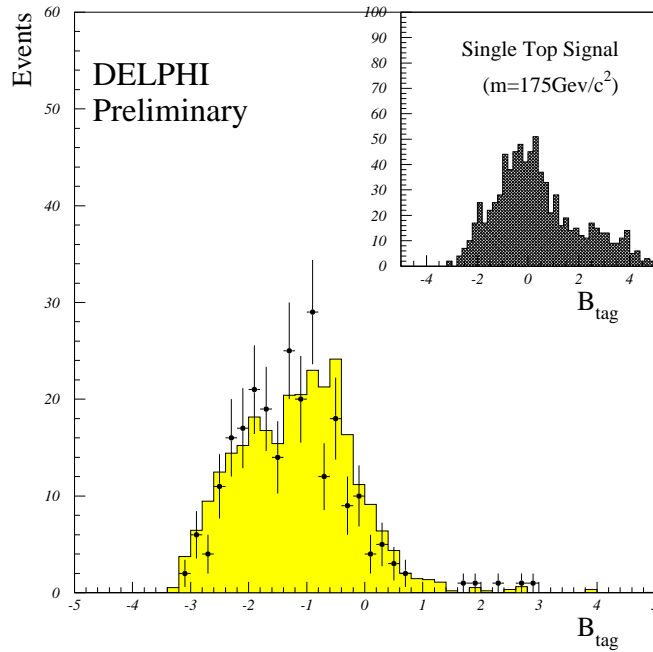


Figure 6: The event combined b-tag variable for the semileptonic decay channel, at a centre of mass energy in the range between 205-207 GeV. The dots show the data, the shadowed region the SM background and the top right distribution a signal of a top with a mass of  $175\text{ GeV}/c^2$ .

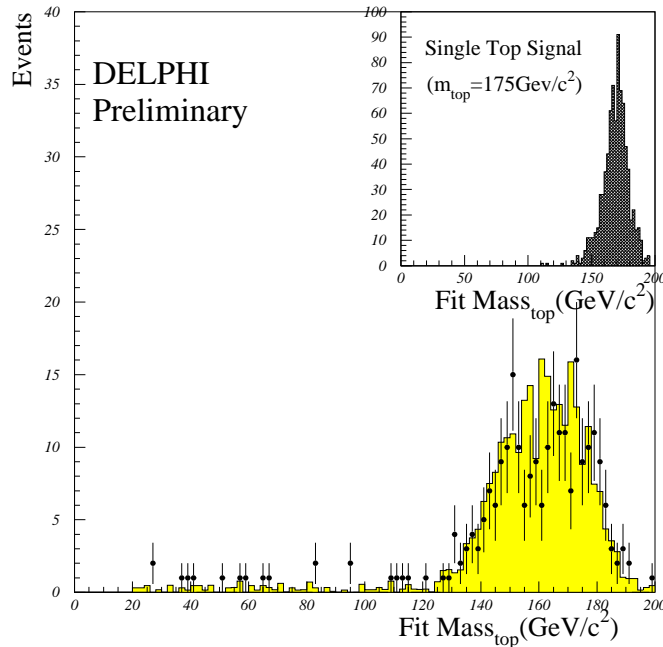


Figure 7: Reconstructed top mass distributions at the pre-selection level for the semileptonic decay channel, at a centre of mass energy in the range between 205-207 GeV. The dots show the data, the shadowed region the SM background and the top right distribution a signal of a top with a mass of  $175\text{ GeV}/c^2$ .

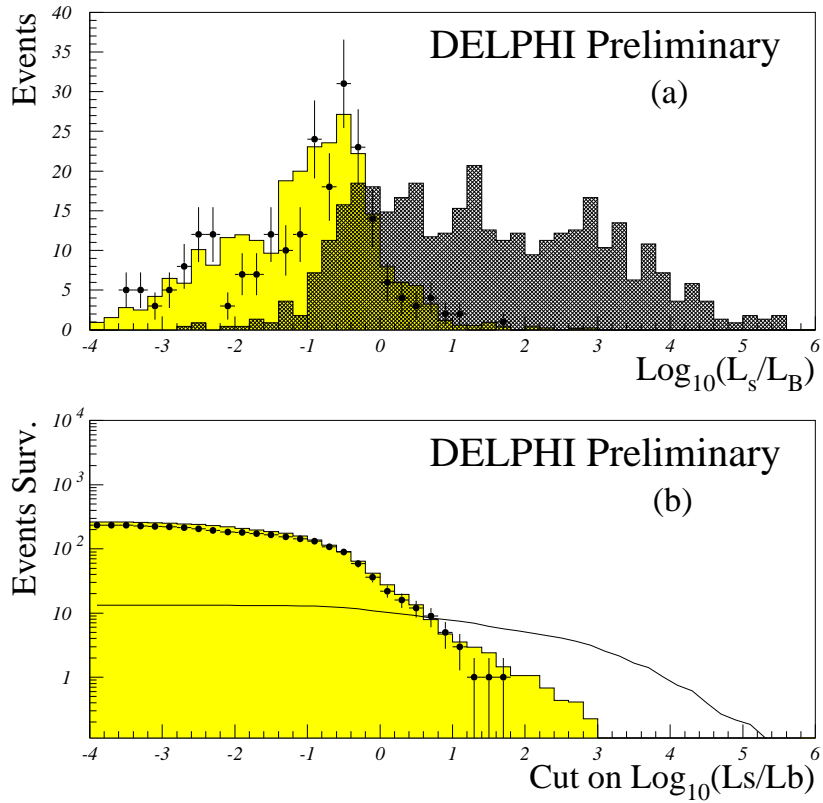


Figure 8: The discriminating variable distribution (a) and the number of events which are accepted in function of the discriminating variable cut (b) for a centre of mass energy ranging from 205 GeV to 207 GeV. The dots show the data, the shaded region the SM simulation and the dark region the expected signal behaviour. In (b) the line represents the signal efficiency convoluted with the  $W$  leptonic branching ratio in function of the discriminating variable cut.

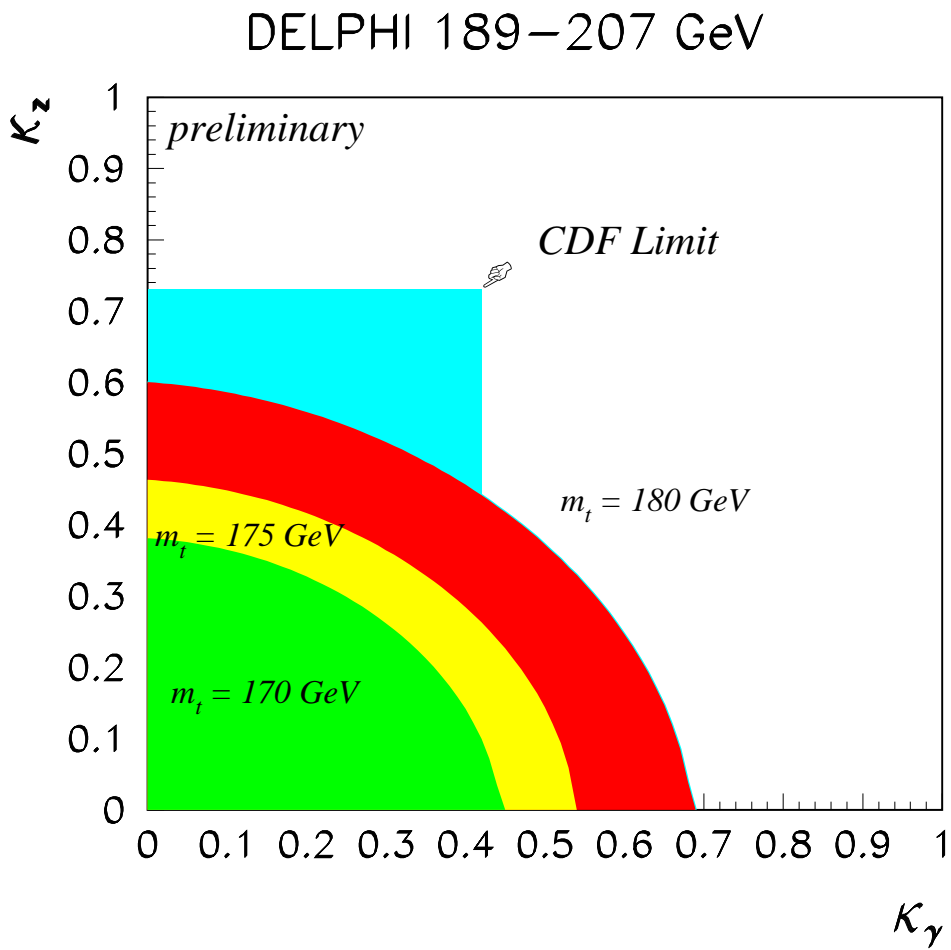


Figure 9: Limits at 95% confidence level in  $\kappa_\gamma - \kappa_Z$  plane. The different areas correspond to different top quark masses.